Global Change Biology

Global Change Biology (2016), doi: 10.1111/gcb.13320

Cold air drainage flows subsidize montane valley ecosystem productivity

KIMBERLY A. NOVICK[1], A. CHRISTOPHER OISHI[2] and CHELCY FORD MINIAT[2]

[1]*School of Public and Environmental Affairs, Indiana University – Bloomington, 702 N. Walnut Grove Avenue, Bloomington, IN 47405, USA,* [2]*USDA Forest Service – Southern Research Station, Coweeta Hydrologic Laboratory, 3160 Coweeta Lab Road, Otto, NC 28763, USA*

Abstract

In mountainous areas, cold air drainage from high to low elevations has pronounced effects on local temperature, which is a critical driver of many ecosystem processes, including carbon uptake and storage. Here, we leverage new approaches for interpreting ecosystem carbon flux observations in complex terrain to quantify the links between macro-climate condition, drainage flows, local microclimate, and ecosystem carbon cycling in a southern Appalachian valley. Data from multiple long-running climate stations and multiple eddy covariance flux towers are combined with simple models for ecosystem carbon fluxes. We show that cold air drainage into the valley suppresses local temperature by several degrees at night and for several hours before and after sunset, leading to reductions in growing season respiration on the order of ~8%. As a result, we estimate that drainage flows increase growing season and annual net carbon uptake in the valley by >10% and >15%, respectively, via effects on microclimate that are not be adequately represented in regional- and global-scale terrestrial ecosystem models. Analyses driven by chamber-based estimates of soil and plant respiration reveal cold air drainage effects on ecosystem respiration are dominated by reductions to the respiration of aboveground biomass. We further show that cold air drainage proceeds more readily when cloud cover and humidity are low, resulting in the greatest enhancements to net carbon uptake in the valley under clear, cloud-free (i.e., drought-like) conditions. This is a counterintuitive result that is neither observed nor predicted outside of the valley, where nocturnal temperature and respiration increase during dry periods. This result should motivate efforts to explore how topographic flows may buffer eco-physiological processes from macroscale climate change.

Keywords: complex terrain, drainage flows, drought, ecosystem respiration, gross ecosystem productivity, microclimate, net ecosystem exchange, net ecosystem productivity

Received 11 October 2015 and accepted 28 March 2016

Introduction

In the more than 30 million km^2 of the terrestrial surface that is mountainous (Kapos *et al*., 2000), topographic features can significantly decouple micro- and macro-climate dynamics (Dobrowski, 2011), where microclimate varies over scales of ~1 km, and macro-climate varies over spatial scales of 10^3 km or more. For example, vegetation in valley positions has been shown to be the beneficiary of hydraulic subsidies, (Weyman, 1973; Crimmins *et al*., 2011; Dobrowski, 2011), whereby water draining downslope through soil matrices enhances productivity by reducing the occurrence of soil moisture limitations to photosynthesis and growth. But water is not the only fluid that flows downhill in mountainous areas. Nocturnal surface cooling promotes the frequent development of a stable layer of cold air that also flows downslope and pools in valleys (Daly *et al*., 2010; Dobrowski, 2011; and see Fig. 1). Cold air drainage and pooling can suppress temperature in valley positions by as much as 5–10 °C (Cox, 1920; Gudiksen *et al*., 1992), promoting the development of temperature inversions characterized by warmer air aloft. In humid landscapes like the southern Appalachian mountains, temperature inversions driven by cold air drainage can often be 'seen' as blankets of fog overlaying low-elevation areas where the air temperature has been lowered below the dew point (Fig. 1c). With this work, we investigate whether downslope cold air subsidies, like downslope soil moisture subsidies, also represent an enhancement to net ecosystem productivity, which is suppressed by high temperatures (Long, 1991).

Drainage flows and cold air pooling occur most frequently at night (Lundquist & Cayan, 2007) and in areas of complex terrain (Chung *et al*., 2006; Hubbart *et al*., 2007), although they can also evolve along relatively shallow slopes (Mahrt *et al*., 2001). Previous work has also suggested that the evolution of drainage flows depends on macroscale climate conditions and specifically that drainage flows tend to evolve more readily under clear sky conditions which promote radiative

Correspondence: Kim Novick, tel. 1 812 855 3010, fax 1 812 855-7802, e-mail: knovick@indiana.edu

surface cooling (Barr & Orgill, 1989; Gudiksen *et al.*, 1992; Daly *et al.*, 2010; and see Fig. 1).

Temperature is a critically relevant variable for a range of eco-physiological processes, including respiration (Reichstein *et al.*, 2005), photosynthesis (Bernacchi *et al.*, 2003), and ontogeny (Bentz *et al.*, 1991; Kramer *et al.*, 2000; Gan, 2004; Thuiller *et al.*, 2005). Previous work has shown that cold air drainage effects on temperature can influence many ecosystem processes, including budburst (Inouye *et al.*, 2000), plant water relations (Hubbart *et al.*, 2007), and seedling regeneration (Blennow & Lindkvist, 2000). However, with a few exceptions (Bolstad *et al.*, 1998; Pypker *et al.*, 2007), studies that link cold air drainage to patterns and trends in ecosystem carbon cycling are scarce. While drainage flows are frequently identified in studies that report observations of ecosystem carbon fluxes, these efforts have historically been focused on the extent to which cold air drainage challenges the interpretation of turbulent flux observations (Lee & Hu, 2002; Mammarella *et al.*, 2007; Leuning *et al.*, 2008; Yi *et al.*, 2008; Aubinet *et al.*, 2010). Specifically, the presence of drainage flows tends to be associated with non-negligible advection of CO_2 and other scalars in the vertical and/or horizontal direction. These advection fluxes are not measured with traditional eddy covariance systems, but must be accounted for to avoid a systematic underestimation of the net ecosystem productivity (NEP).

Recently, methodological advances to observe or infer the magnitude of advection fluxes (Lee & Hu, 2002; Mammarella *et al.*, 2007; Leuning *et al.*, 2008; Feigenwinter *et al.*, 2010; Novick *et al.*, 2014) permit a more confident interpretation of ecosystem-scale fluxes in complex terrain. The work reported here builds upon a recent and exhaustive effort to apply these techniques to characterize the advection flux regime at an Appalachian valley flux monitoring site situated in the Coweeta Hydrologic Laboratory (North Carolina, USA, Novick *et al.*, 2014). That work concluded that periods of significant advection in the Coweeta site, which tend to occur during the hours of midnight and sunrise, can be reliably identified and filtered.

Our work is oriented around the prediction that cold air drainage will enhance net ecosystem productivity in the valley, predicated on the expectation that air temperature will be relatively high in valley positions during daytime periods, but relatively cool at night, as previously reported by Bolstad *et al.* (1998) and illustrated in Fig 1. To test this prediction, we will answer a series of specific research questions:

1. By how much, and for what periods of the day, does cold air drainage reduce nocturnal temperature in the valley, when compared to higher elevation positions and the region at large?
2. By what magnitude do temperature reductions in the valley affect ecosystem respiration, gross ecosystem productivity, and NEP?
3. To what extent is the evolution of drainage flows linked to macro-climate condition, and what are the

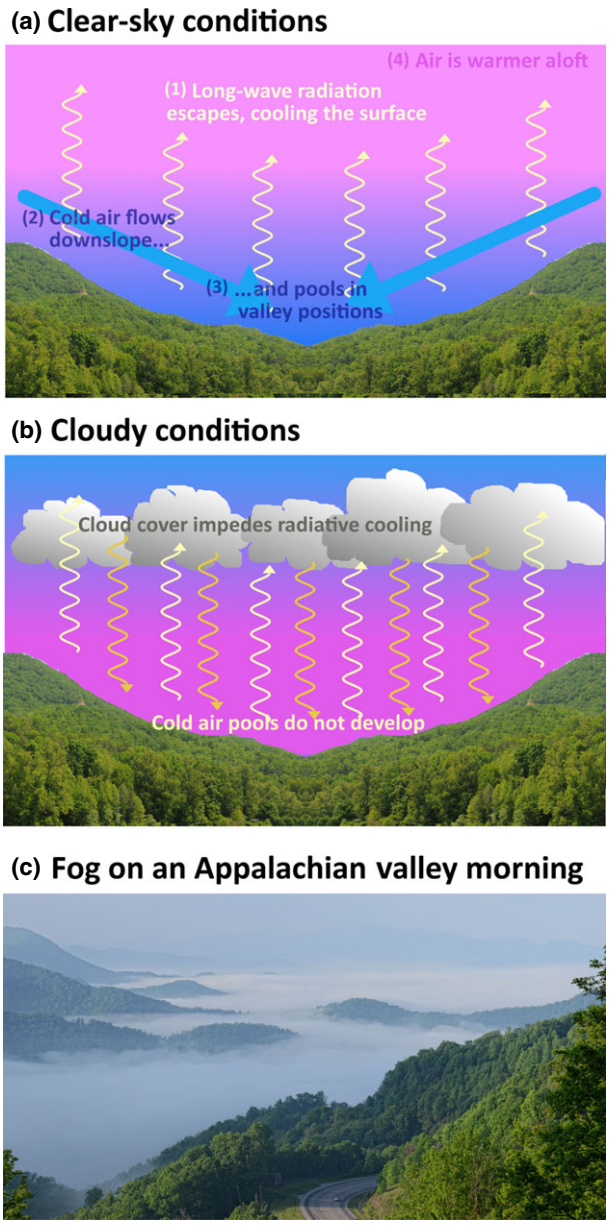

Fig. 1 A conceptualization of how cold air drainage proceeds under low humidity conditions (a), but is impeded by cloud cover (b). Panel (c) shows a photograph of a southern Appalachian valley taken shortly after sunrise. The effect of cold air drainage on the dew point in valley positions can be seen as low-elevation fog cover. Photograph in (c) by Eric Haggart.

carbon cycle consequences of these interactions between macro-climate and cold air drainage?

This work is further motivated by the fact that effects of topographic flows on carbon cycling are not well represented in terrestrial ecosystem models (Rotach *et al.*, 2014), which tend to operate over spatial scales that are coarser than those over which topography-driven variation in microclimate evolves (Daly, 2006; Holden *et al.*, 2011; Ashcroft & Gollan, 2012). Thus, links between drainage flows, and micro- and macro-climate dynamics in complex terrain have historically neither been routinely measured nor adequately represented in models and thus represent an important knowledge gap in our understanding of ecosystem carbon cycling in complex terrain.

Materials and methods

Study area

The experiment was conducted in the southern Appalachian mountains at the Coweeta Hydrologic Laboratory (35.059N, 83.427W, 690–1600 m a.s.l.). Coweeta is a USDA Forest Service Experimental Forest, and National Science Foundation Long-Term Ecological Research (LTER) site. The primary study ecosystem is an ~85-year-old, mixed deciduous hardwood forest located in a sheltered valley at the base of the Coweeta Basin. An eddy covariance flux monitoring tower has been operational in the valley position since 2011. The tower is situated in complex, mountainous terrain characterized by a 30% slope within the flux footprint in the SE direction, and local slopes of <10% to the NE and SW (Fig. 2a). Mean annual temperature is 12.9 °C and mean annual precipitation is 1795 mm. Observed micro-climate dynamics in the valley position are compared to observations collected at other, higher elevation locations in the valley, and also to observations collected across the broader region (Fig. 2a, b). Carbon fluxes in the valley are compared to those collected from a second flux tower located in the Duke Forest in the central North Carolina piedmont (Fig. 2b). The piedmont site is the Duke Hardwood forest Ameriflux site (35°58′41″N, 79°05′59″W, 163 m a.s.l.), which is also an ~80-year-old deciduous hardwood forest. The latitudes at the Coweeta and Duke Forest locations are similar, but the Duke site is located on relatively flat terrain that does not experience significant cold air pooling. All data analyses were limited to the growing season (April–September), which is most relevant for eco-physiological functioning in temperate deciduous forests.

Climate station observations within and outside the Coweeta basin

Hourly averaged air temperature, incident short-wave radiation (R_g), and vapor pressure deficit (D) were recorded a climate station located in the Coweeta valley within 200 m of the flux tower (CS01). Hourly averaged air temperature and D were also recorded at four other climate stations within the Coweeta basin spanning an elevation range of >700 m, as described in Laseter *et al.* (2012). The main text of this study was focused comparing data recorded at CS01 to data recorded at a station located in a mid-slope position (CS17, Fig. 2a) that is separated from CS01 by 200 m and 2 km in the vertical and lateral directions. Data from the other stations appear in supporting analyses contained in the supplementary information (hereafter the SI). The dynamics of air temperature, D, and radiation in the Coweeta basin were further compared to observations of those same variables obtained from seven meteorological stations located at lower elevations outside of the Coweeta Basin. They include five stations managed as part of the North Carolina Climate Retrieval and Observations Network of the Southeast (CHRONOS, http://www.nc-climate.ncsu.edu/) database, plus an additional two stations maintained as part of the US Climate Reference Network (USCRN, http://www.ncdc.noaa.gov/crn/). The stations were selected for their proximity to Coweeta (40–200 km), the completeness of their data records, and because they are located on the same side as the Appalachian mid-continental divide as Coweeta. Analysis of all climate station data was also limited to the growing season during the period from 2011–2013.

Observations of soil temperature

Soil temperature was measured continuously from 2011–2013 at depths of 5 and 20 cm at several locations within the Coweeta tower footprint. It was also measured at depths of 5 and 20 cm in the mid-slope position at a 300-m lateral (i.e., along-slope) distance from CS17. In each location (i.e., valley and mid-slope), soil temperature was averaged hourly over all monitoring locations, producing soil temperature time series representative of the top 20 cm of the soil.

Eddy covariance observations of NEP and associated meteorological variables

Hourly averaged eddy covariance fluxes of the net ecosystem productivity (NEP) were recorded on the Coweeta flux tower from 2011–2013. Turbulent fluxes were measured with an EC-155 enclosed path gas analyzer (Campbell Scientific, Logan, Utah, USA) and a sonic anemometer (RM Young 8100, RM Young, Traverse City, MI) as described in detail in Novick *et al.* (2013). Flux observations at Coweeta are often challenged by advection flows and flux footprint inconsistencies, and the analysis herein relies only on data that have been rigorously quality controlled. Specifically, data are limited to those collected when wind originates from a direction characterized by consistent forest cover and reliable wind characteristics (220–310° from N) and excludes time periods known to be associated with large advection fluxes and low turbulent fluxes (Novick *et al.*, 2014). Turbulent flux data were corrected for within-canopy storage calculated from a vertical gas and temperature profiling system.

A number of meteorological and hydrologic variables were also recorded hourly on the tower, including incident short- and long-wave radiation (R_g and R_{LW}, respectively, CNR1,

Kipp & Zonen, Delft, The Netherlands), and soil moisture content (CS616, Campbell Scientific). The integrated soil moisture over the top 30 cm was measured at four locations within the tower footprint.

The Duke Forest Hardwood Site Ameriflux tower was operational from 2001–2008 (Stoy *et al.*, 2008). Eddy covariance fluxes and associated meteorological variables were measured using a LI-7500 open path gas analyzer (Li-Cor Biogeosciences, Lincoln, NE) and a sonic anemometer (CSAT 3, Campbell Scientific). Quality control for these data and the associated meteorological variables are described in detail in Novick *et al.* (2015).

Parameterizing simple models from the components of NEP

The temperature dependence of ecosystem respiration (RE) was modeled as:

$$\mathrm{RE} = R_{\mathrm{ref}} \times Q^{aT_{\mathrm{air}}+B} \quad (1)$$

The parameters a and b were set to 0.1 and −2, respectively, after Tjoelker *et al.* (2001). The reference respiration rate (R_{ref}, μmol m^{-2} s^{-1}) and the temperature sensitivity parameter Q (unitless) were set as free parameters to be determined by the observations. The gross ecosystem productivity (GEP) was assumed to be a function of R_g and D using a model proposed by Lasslop *et al.* (2010):

$$\mathrm{GEP} = \frac{\alpha\beta R_g}{\alpha R_g + \beta}, \quad (2)$$

where α is the mean apparent ecosystem quantum yield, and β is the maximum assimilation rate. When $D > 1$ kPa, the β is modified according to

$$\beta = \beta_0 \exp[-k(D-1)] \quad (3)$$

where β_o is a reference assimilation rate at low D, and k is the humidity response parameter.

Unique, site-specific parameterizations for Eqn 1 were achieved for Coweeta and the Duke Forest using nonlinear regression in MATLAB (Mathworks, Natick, MA). We limited the data driving the regression to all available nocturnal data collected when soil moisture was between 0.3 and 0.46 m^3 m^{-3} in Coweeta, and between 0.2 and 0.4 in the Duke Forest, as RE was determined to be largely insensitive to soil moisture within those ranges (data not shown).

Equation 1 was then forced with the locally observed T_{air} time series to generate a continuous estimate of *RE*, which was subtracted from the observed, quality-controlled NEP to obtain an estimate of GEP. The GEP estimates were then used to parameterize Eqns 2 and 3 for each site, again using nonlinear regression in MATLAB. 95% confidence intervals were determined for the parameters using a nonparametric bootstrap with 1000 iterations. Parameters were generally similar between the sites (see Table 1).

Proxies for cold air drainage

We considered two proxies for the intensity of cold air drainage into the valley. The first was the mean difference in air temperature between the CS01 (valley) and CS17 (midslope) climate stations (hereafter T_{VALLEY} - T_{MIDSLOPE}), noting that analyses based on other climate stations in the Coweeta Basin produced similar results (see Appendix S1 of the SI). In the absence of cold air drainage, we would expect that $T_{\mathrm{VALLEY}} - T_{\mathrm{MIDSLOPE}}$ should always be positive (i.e., the lower elevation valley is warmer). We would further expect $T_{\mathrm{VALLEY}} - T_{\mathrm{MIDSLOPE}}$ to be highest during midday periods, when the pressure-driven lapse rate may be more similar to the dry adiabatic lapse rate (~10 °C/km, Bolstad *et al.*, 1998) then it would be at night, when relatively humidity is close to 100% and the wet adiabatic lapse rate (~4 °C/km,, Bolstad *et al.*, 1998) likely applies.

A second proxy for cold air drainage is the difference in nocturnal temperature in the valley and the broader region (hereafter T_{VALLEY} - T_{REGION}), where T_{REGION} is the mean air temperature observed among the seven meteorological stations located <200 km from Coweeta (Fig. 2b). When comparing the Coweeta basin to the region at large, we would again expect Coweeta Basin to always be cooler than the surrounding region (as the basin is located at a higher elevation, see SI). In the absence of cold air drainage, we would expect the valley to be coolest during the daytime, when air is drier and the adiabatic lapse rate is steeper. In support of this analysis and all analyses for which the difference between two variables is assessed, the significance of mean difference between two variables is determined from a two-tailed Student's t-test for the different of the means. Results of the t-test are reported as *P*-values.

Disentangling radiation and cold air drainage effects on temperature

The $T_{\mathrm{VALLEY}} - T_{\mathrm{REGION}}$ is sensitive to variation in local radiation driven by patterns of orographic precipitation. We used a radiation balance model to disentangle the effects of solar radiation and cold air drainage on the observed $T_{\mathrm{VALLEY}} - T_{\mathrm{REGION}}$. Following the arguments presented in Juang *et al.* (2007) and Luyssaert *et al.* (2014), the expected change in surface temperature (ΔT_s) for a given change in incident short-wave solar radiation (ΔR_g) and/or incident long-wave solar radiation (ΔR_{LW}) may be expressed as:

$$\Delta T_S = \frac{1}{4\sigma T_S^3 + \eta}[(1-\alpha)\Delta R_g + \Delta R_{\mathrm{LW}}] \quad (4)$$

Here, σ is the Stefan-Boltzmann constant, α is albedo, and the parameter η incorporates aerodynamic and ecophysiological controls on sensible and latent heat fluxes (Juang *et al.*, 2007). The α was assumed to be 0.20 and η was assumed to be 40 W m^2 K^{-1}, which are typical growing season values for the southeastern U.S. grasslands that typically underlie climate monitoring stations (Juang *et al.*, 2007). The ΔR_g was determined as the difference in solar radiation measured at CS01 and the mean solar radiation observed across the network of meteorological stations. Long-wave radiation was observed on top of the Coweeta flux tower, and was not observed at the regional meteorological stations. Thus, ΔR_{LW} was estimated from an

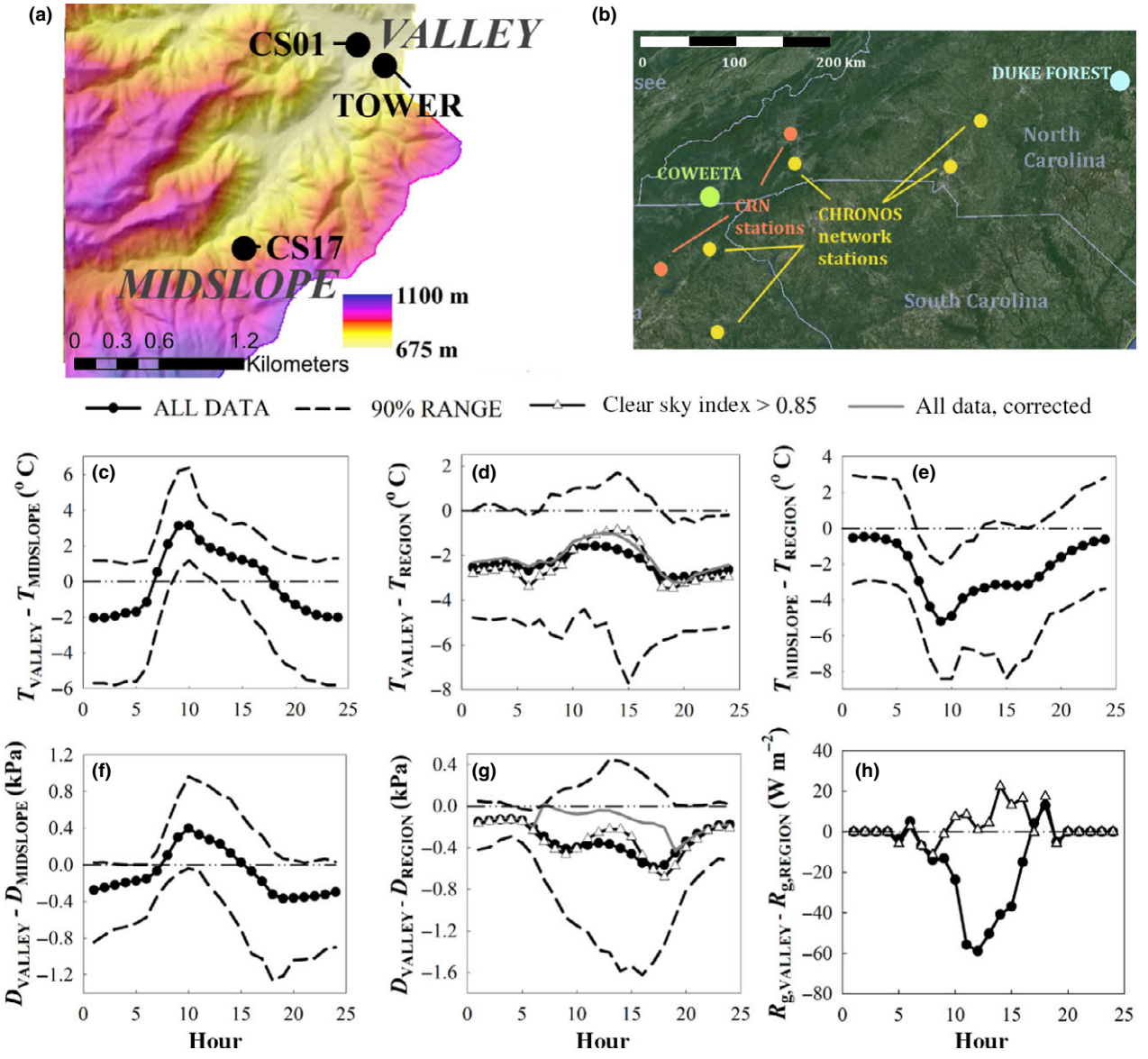

Fig. 2 Map of Coweeta Basin (a) showing the eddy flux tower and climate stations (i.e., CS01 and CS17), and (b) the regional climate stations and the Duke Forest flux tower. Panel (c) shows the difference in growing season air temperature between the valley and mid-slope position. In panel (d), the difference in regional mean ambient surface air temperature from CS01 is shown (circles) alongside the same data collected on sunny days only (triangles) and after applying a correction for differences in temperature attributable to differences in incident solar radiation (gray line). Panel (e) shows the difference between air temperature measured in the mid-slope position and the region at large. Panels (f) and (g) illustrate differences in vapor pressure deficit between the valley and mid-slope position, and the valley and the region at large, respectively. Panel (h) illustrates the difference in short-wave radiation between the valley and the region for all growing season periods (black circles) and sunny days only (open triangles).

empirical relationship between incident short- and long-wave radiation measured on the Coweeta tower, as described in detail in the SI, noting that in general the ΔR_{LW} effects on ΔT_s were small.

To test the functionality of the model, we compared the corrected $T_{VALLEY} - T_{REGION}$ to the $T_{VALLEY} - T_{REGION}$ observed on days when the valley and region were relatively cloud-free. To identify clear days, we used a 'clear sky index' defined as the daily-averaged ratio of the observed R_g to the theoretical maximum incident shortwave radiation under cloud-free conditions ($R_{g,max}$):

$$\text{Clear Sky Index} = R_g/R_{g,max}(\text{daily-averaged}) \quad (5)$$

The $R_{g,max}$ was calculated as the sum of the beam and diffuse irradiance on a horizontal surface as described in Appendix S3 of the SI.

Table 1 The parameters of the models for gross ecosystem productivity and ecosystem respiration (Eqns 1–3). Numbers in parentheses show 95% confidence intervals for the Coweeta parameters, as derived from a nonparametric bootstrap with 1000 iterations. Data availability is higher at Duke Forest (n = 5000 and 2500 hourly observations to parameterize Eqns 1–3, respectively) compared to Coweeta, where the record is shorter and filtering to remove observational bias driven by topography and footprint constraints is extensive ($n \approx 1000$ hourly observations of RE and GEP). Thus, confidence intervals on the Duke Forest parameters are very small and not shown

	α μmol J^{-1}	β_o μmol m^{-2} s^{-1}	k	R_{ref} μmol m^{-2} s^{-1}	Q
Coweeta	0.077 (0.070–0.0842)	36.4 (32.5–40.6)	0.10 (0.02–0.18)	3.65 (3.26–4.03)	2.08 (1.54–2.74)
Duke Forest	0.101	42.6	0.11	5.59	1.62

Direct observations of cold air drainage effects on ecosystem respiration

Direct observations of the effect of cold air drainage on ecosystem-scale fluxes are challenged by the fact that periods of intense cold air drainage typically occur coincident with periods of significant advection of CO_2 into the flux tower footprint. However, there does exist a small window of time in the early evening between sunset and midnight when drainage flows may already be affecting temperature dynamics, but vertical and horizontal advection of CO_2 is still minimal, such that the total NEP (which during this time period is dominated by RE) may be accurately estimated from the sum of turbulent and storage flux observations (van Gorsel *et al.*, 2009; Novick *et al.*, 2014). Thus, to demonstrate a direct effect of cold air drainage on RE, we bin all available data collected between sunset and midnight according to the intensity of cold air drainage using $T_{VALLEY} - T_{MIDSLOPE}$ as a proxy, and average the RE observations within each bin. We limit this analysis to data collected when soil moisture was between 0.30 and 0.46 m^3 m^{-3} to avoid any confounding effects from soil moisture limitations.

Utilizing ecosystem-scale models to quantify drainage flow, lapse rate, and radiation effects on carbon fluxes

We complement direct observations of drainage flows with a modeling exercise to infer the effects of not only drainage flows, but also elevation-driven lapse rate and radiation gradients, on RE, GEP and NEP over the course of a representative 24-h growing season period.

Toward that end, we forced the model of Eqn 1, parameterized for the Coweeta site, with (i) the observed valley temperature, (ii) the regional temperature time series, (iii) the regional temperature time series after correcting for the regional lapse rate (taken to be 5.5 °C km^{-1}, after Bolstad *et al.*, 1998), and (iv) the regional time series after correcting for differences in radiation between the valley and the region using Eqn 4.

A complimentary analysis was performed to explore the effect of drainage flows on GEP. After parameterizing the GEP model of Eqns 2 and 3 (see Table 1), we forced the model with the observed regional R_g and D time series. We also forced the model with estimates of D adjusted for lapse rate and radiation effects by modifying the saturation vapor pressure with corrected temperature series. The modeled estimates driven by the various meteorological time series were then averaged over the growing season according to time of day.

Exploring links between macro-climate condition, drainage flows, and local microclimate and carbon cycling

Drainage flows have been reported to proceed more readily under clear, dry macro-climate conditions (Gudiksen *et al.*, 1992). To explore the links between increasingly dry macroclimate, drainage flows, and carbon fluxes in our study area, we used Eqns 1–3 to predict the dynamics of NEP, RE, and GEP inside and outside of the valley along a gradient of increasing D. When predicting the dynamics of NEP, RE and GEP, the mid-slope position was taken as representative of positions outside of the valley to avoid complications driven by spatial variation in radiation between the valley and the region at large.

The predicted patterns for NEP along the gradient of increasing D were compared to NEP observed in the Coweeta valley and the Piedmont tower sites. For the cross-site comparisons of trends in the predicted and modeled carbon fluxes along the D gradient, variables were normalized by their mean growing season value at low D (D < 0.2 kPa) to account for other factors besides drainage flow that might drive differences in carbon fluxes between the Coweeta valley and the Piedmont tower sites.

Sensitivity of leaf and soil temperature and respiration to drainage flow effects

A more mechanistic understanding of drainage flow effects on ecosystem respiration may be achieved by understanding how drainage flows independently affect the respiration of soil as compared to aboveground biomass. Toward that end, we assume that soil respiration is driven primarily by soil temperature, whereas respiration of aboveground biomass, and especially leaves, should be more closely coupled to air temperature. Observations of both soil and leaf temperature from the valley and midslope position were then integrated into previously published models for soil and leaf respiration developed using leaf- and chamber-level observations in the Coweeta basin (Mitchell *et al.*, 1998; Nuckolls *et al.*, 2009). The models have the same form as Eqn 1, that is:

$$R_{i,j} = R_{\mathrm{ref},i,j} Q_{i,j}^{a_i T_{k,j} + b_i} \quad (6)$$

where the subscript i indicates either 'soil' or 'leaf', the subscript j indicates topographic position (valley or midslope), and the subscript k indicates either soil temperature (in the case of soil respiration) or air temperature (in the case of leaf respiration). Following Nuckolls *et al*. (2009), a_{soil} was set to 0.152 and b_{soil} was set to 0. Following Mitchell *et al*. (1998), a_{leaf} was set 0.10 and b_{leaf} was set to −2 (analogous to the parameterization for ecosystem respiration).

We considered two scenarios in this modeling exercise, with two unique analysis goals. In the first scenario, our objective was to isolate the effects of cold air drainage on the diurnal evolution of soil and leaf respiration in the valley as compared to the midslope position. Observations of soil and air temperature data from the mid-slope position were corrected for the local lapse rate (i.e., 5.5 °C km^{-1}, Bolstad *et al*., 1998), and we assumed that R_{ref} and Q were unchanged between the valley and midslope position. In this case, the relative respiration rate (i.e., $R_{i,\mathrm{VALLEY}}/R_{i,\mathrm{MIDSLOPE}}$) becomes:

$$\text{Relative } R_i = \frac{Q_i^{a_i T_{k,\mathrm{VALLEY}} + b_i}}{Q_i^{a_i T_{k,\mathrm{MIDSLOPE}} + b + {}_i}} \quad (7)$$

Bolstad *et al*. (1999), who synthesized leaf-level chamber-based measurements of the dark respiration rate from across the Coweeta Basin, reported that the Q_{leaf} of the four most dominant species in the Coweeta valley flux tower footprint (*Acer rubrum*, *Quercus alba*, *Betula lenta*, and *Liriodendron tulipifera*) ranged from 2.2 to 2.6. For the purposes of this exercise, the 'canopy-averaged' Q_{leaf} was set to 2.3. After Nuckolls *et al*. (2009), who synthesized chamber-based soil CO_2 efflux observations from across the Coweeta basin, Q_{soil} was set to 2.71 (i.e., *e*).

The objective of the second modeling scenario was to explore the extent to which acclimations or adaptations to the R_{ref} or Q across the elevation gradient might affect the relative respiration rate, which in this case may be expressed as:

$$\text{Relative } R_i = \frac{R_{\mathrm{ref},i,\mathrm{VALLEY}}}{R_{\mathrm{ref},i,\mathrm{MIDSLOPE}}} \times \frac{(Q_{i,\mathrm{VALLEY}})^{a_i T_{k,\mathrm{VALLEY}} + b_i}}{(Q_{i,\mathrm{MIDSLOPE}})^{a_i T_{k,\mathrm{MIDSLOPE}} + b_i}} \quad (8)$$

In the Coweeta basin, the $R_{\mathrm{ref,leaf}}$ increases by up to 40% over an elevation change of 1000 m (Mitchell *et al*., 1998; Bolstad *et al*., 1999), representing an acclimation among plants growing in cooler, higher elevation environments (Bolstad *et al*., 1999). As the elevation change between the valley and midslope position is 0.2 km, we set the ratio of $R_{\mathrm{ref,leaf,valley}}$: $R_{\mathrm{ref,leaf,midslope}}$ to 0.9, representing a ~10% increase between the valley and midslope. No direct estimates for the rate of change of Q_{leaf} with elevation in the Coweeta basin are available, although other work suggests that Q_{leaf} increases in cooler biomes by a rate of about 10% for every 5 degree increase in measurement temperature (Tjoelker *et al*., 2001). Thus, we retain $Q_{\mathrm{leaf,valley}} = 2.3$, but set $Q_{\mathrm{.leaf,midslope}} = 2.4$, consistent with a ~1–2 °C temperature shift between the valley and midslope positions predicted from the regional lapse rate. In the absence of direct observations of the change in $R_{\mathrm{ref,soil}}$ *and* Q_{soil} with elevation in the Coweeta basin, these parameters were assumed to vary between sites in a manner similar to variation in the leaf respiration parameters. Specifically, $R_{\mathrm{ref\ soil,valley}}$:$R_{\mathrm{ref,soil,midslope}}$ was also set to 0.9, and the $Q_{\mathrm{soil,midslope}}$ was increased to 2.8. For this second modeling scenario, the leaf and soil temperature time series were not corrected for lapse rate effects.

Soil moisture effects on soil respiration were not considered in this modeling exercise. Justification for this omission comes from previous work finding that soil moisture limitations were rare in the Coweeta basin and typically reduced R_{soil} by < 3% (Nuckolls *et al*., 2009). While no data exist from which to infer soil limitation to R_{leaf} directly, we can assume that soil moisture will generally be lower at higher elevations, as downslope positions receive moisture subsidies. The fact that $R_{\mathrm{ref,leaf}}$ increases as elevation increases (Mitchell *et al*. 1998) could be taken as an indication that soil moisture constraints to R_{leaf} at high elevation are not large. Nonetheless, they may exist, which would have the effect of increasing the relative respiration rate.

Results

Variation in microclimate conditions between the valley, the mid-slope position, and the region at large

Consistent with expectations based on lapse rate effects, we find that during daytime periods, mean daytime $T_{\mathrm{VALLEY}} - T_{\mathrm{MIDSLOPE}}$ in the Coweeta Basin was between 0.7 and 1.8 °C, indicating that the valley was warmer than the mid-slope position (Fig. 2c, $P < 0.005$ for the difference in the mean of all data collected at each location between 800 and 1600 h). However, at night, the mean nocturnal $T_{\mathrm{VALLEY}} - T_{\mathrm{MIDSLOPE}}$ was negative ~80% of the time, and was −2 °C on average, indicating the influence of cold air drainage (Fig. 2c, $P < 0.0001$ the difference in the mean of all data collected at each location before 700 h and after 1900 h).

When comparing the Coweeta basin to the region at large, we find that T_{VALLEY} was generally cooler than the region, consistent with expectations based on lapse rate effects, but it was particularly depressed at night (Fig. 2d, $P < 0.0001$), which is not expected from lapse rate considerations and again indicates cold air drainage. On relatively clear days, air temperature in the Coweeta Valley was more similar to the region at large, but on clear nights, air temperature in the valley was suppressed even further (Fig. 2d, open triangles, $P < 0.0001$). After accounting for the effects of suppressed solar radiation in the Coweeta Basin (see methods), the $T_{\mathrm{VALLEY}} - T_{\mathrm{REGION}}$ was more similar to that observed under clear conditions (Fig. 2d, gray line) during daytime, but less similar during nighttime, which is a first indication that cold air drainage proceeds more readily in the Coweeta basin under clear sky conditions. The difference between temperature in the midslope position and the region at large was also

generally negative ($P < 0.0001$ for both daytime and nighttime periods), and as expected in the absence of a cold air drainage effect, the $T_{MIDSLOPE}$ - T_{REGION} was lowest during daytime periods (Fig. 2e).

The nocturnal vapor pressure deficit in the valley, which is strongly determined by the local temperature, was also generally lower than the midslope (Fig. 2f, $P < 0.0001$), and almost always lower than the surrounding region (Fig. 2g, $P < 0.0001$). Solar radiation tended to be suppressed in the Coweeta valley most days, representing the action of orographic rainfall and early morning fog events (Fig. 2h), although the result was not significant at the 95% confidence level ($P = 0.16$).

It is interesting to note that the mean nocturnal $T_{MIDSLOPE}$ - T_{REGION} (usually >−1 °C) was actually higher than that predicted by the wet adiabatic lapse rate (i.e., −2 °C, see Fig. 2e), which could indicate a compensating effect of cold air drainage whereby removal of cold air upslope elevates nocturnal temperature. However, an analysis of other climate stations in the Coweeta basin reveals that in some cases, the nocturnal temperature patterns were very well matched with those predicted from lapse rate considerations (see SI). Moving forward, we will focus our analysis on the extent to which cold air drainage affects temperature, and thus carbon cycling, in the valley position, although we will return to the possibility of compensating effects in the discussion.

Direct observations of the drainage effect on ecosystem respiration

As the intensity of cold air drainage increased (defined as increasingly negative $T_{VALLEY} - T_{MIDSLOPE}$), the observed NEP during the period between sunset and midnight decreased (Fig. 3). As NEP is dominated by respiration during this time window, this result offers direct observational evidence for suppression of RE by cold air drainage. To ensure that this decline in RE is a mechanistic response, and not an artifact of the tendency of flux observations to be underestimated during periods of significant CO_2 advection, we predicted the RE in each drainage flow class using Eqn 1 forced with the air temperature observed at either CS01 (valley) or CS17 (midslope), with uncertainty on these predictions generated by the range of R_{ref} and Q presented in Table 1. Predictions are well aligned with the observations, indicating that the observed decline in late-evening NEP under high-intensity drainage is explainable primarily by variation in temperature between the valley and midslope position, and is not an artifact of biases in the data themselves. Data considered in this analysis were filtered to within a relatively narrow range of soil moisture, although the results are conserved even when the soil moisture filter is removed. Or, in other words, this result does not represent greater soil moisture limitation when drainage flows are more intense.

Quantifying drainage flow, lapse rate, and radiation effects on carbon fluxes

Via its effect on temperature, we estimate that cold air drainage reduced growing season RE in the valley by ~8.1% (Fig. 4), with a range of 4.5–13.0% determined from the uncertainty on model parameters presented in Table 1. This relative reduction to RE amounts to about 66 g C m^{-2} per growing season (range of 37–107 g C m^{-2}). The lapse rate and radiation effects accounted for an additional 39 g C m^{-2} (range of 20–66 g C m^{-2}, or 2.4–8.1%) and 14 g C m^{-2} (range of 7–24 g, or 1.7–3.0%) reduction to growing season RE (Fig. 4), respectively.

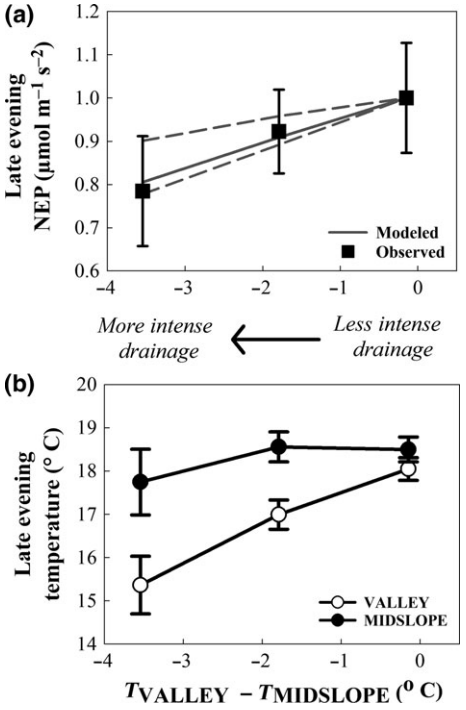

Fig. 3 Panel (a) shows the 'late-evening' (sunset–midnight) NEP as a function of late-evening *T*valley–*T*midslope, where the latter becomes more negative during more intense drainage flow events. Data are shown relative to those observed during the period of least intense drainage. The solid gray line in panel (a) shows the predicted change in NEP with drainage intensity as determined from the model of Eq. 1, driven by the air temperature trends in the valley and the mid-slope that are illustrated in panel (b) for reference. Dashed lines show the range of uncertainty in the prediction determined from the uncertainty in the parameters given in Table 1.

The difference in predicted GEP for the valley as compared to the region was negligible, as increases in regional GEP linked to greater incident radiation tended to be offset by decreases in GEP driven by stomatal closure under higher D. As a result, the ~8% (or 66 g) reduction in growing season averaged RE attributable to cold air drainage translated to a 10% (range of 6–16%) increase in net growing season carbon uptake (i.e., |NEP|). The enhancement to net annual carbon update due to growing season drainage flow effects is estimated to be even larger (17%, range of 10–27%), even without accounting for addition reductions RE due to drainage flows during the dormant season.

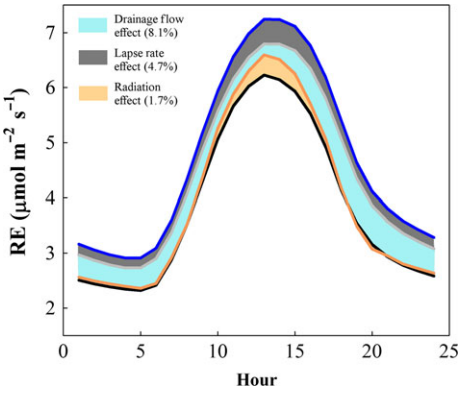

Fig. 4 The mean growing season ecosystem respiration (RE) as a function of time of day. The thick black line represents the model of Eq. 1 as forced with the temperature observed in the Coweeta Valley at CS01. The blue line represents modeled RE as forced with the broader regional temperature. The light grey and orange lines represent the RE forced with regional temperature after correcting for lapse rate and incident solar radiation effects, respectively. The area between the curves corresponds to differences in RE linked to the various physical mechanisms identified in the legend.

Sensitivity of leaf and soil respiration to drainage flows

Suppression of ecosystem respiration (RE) was mainly a function of drainage flows reducing air temperature and thus foliar respiration, rather than drainage flows affecting soil temperature and thus soil respiration. After correcting for lapse rate effects, the difference in air temperature between the valley and mid-slope position regularly exceeded several degrees, whereas the difference in lapse rate corrected soil temperature was typically on the order of 0.5 °C or less (Fig. 5a, b). Soil temperature in the valley was suppressed for a longer period of the day, reflecting the capacity of soil to store and conduct heat (Fig. 5a).

The nocturnal relative soil and leaf respiration rates were typically <1.0, indicating suppression of respiration by cold air drainage. The effect was greater on leaf- compared to soil respiration, with relative R_{soil} on the order of 0.95 compared to relative R_{leaf}, which was on the order of 0.8 for most nocturnal periods (Fig. 5c, d). This result emerges from both modeling scenarios, where again the first scenario was designed to isolate drainage flow effects, and the second was designed to explore the extent to which adaptive R_{ref} and Q might alter the relative respiration rates. The high R_{leaf} observed from approximately 0800 to 1200 h likely represented aspect effects, as the valley position receives more sunlight in the morning than the north-facing mid-slope location. The principle difference between the two modeling scenarios was limited to daytime relative R_{leaf} estimates, when the assumption that $R_{ref,leaf}$

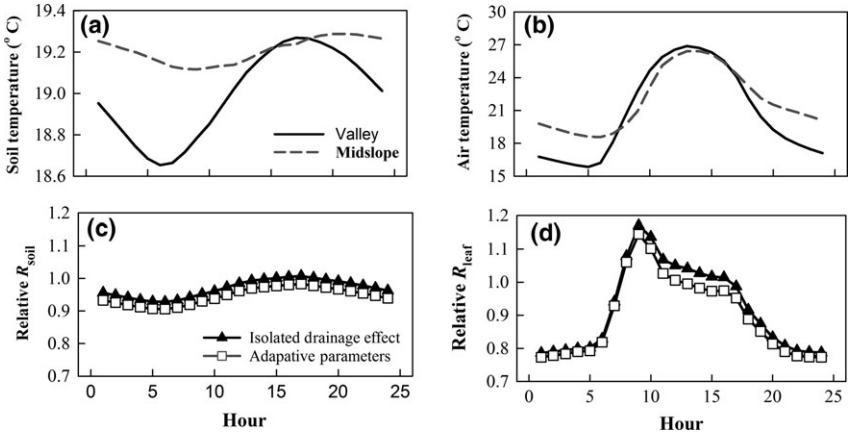

Fig. 5 Panels (a) and (b) show the typical evolution of growing season soil and air temperatures, respectively, in the valley and mid-slope positions. These data have been corrected for lapse rate effects using the local lapse rate of 5.5 °C km^{-1} (Bolstad *et al.*, 1998), which is intermediate between the wet (4 °C km^{-1}) and dry (10 °C km^{-1}) adiabatic lapse rates. Panels (c) and (d) show the evolution of the relative (valley: midslope) soil and leaf respiration rate, respectively. Black triangles show the relative respiration estimated from Eq. 7, and open squares show relative respiration estimated from Eq. 8.

and Q_{leaf} increase in the midslope position increases the midslope R_{leaf} during the day.

Macro-climate and cold air drainage

Drainage flows proceeded more readily under clear and dry macro-climate conditions. Mean nighttime $T_{VALLEY} - T_{MIDSLOPE}$ was most closely coupled to the clear sky index (Fig. 6a), the daily average D (Fig. 6b), and the daily average difference between incident and outgoing long-wave radiation ($r^2 > 0.2$ and $P < 0.0001$ for all variables, see Table 2) observed in the valley position on the days preceding each nocturnal period. The relationships between $T_{VALLEY} - T_{MIDSLOPE}$ and the incident long- and short-wave radiation observed in the valley were also significant ($P < 0.025$) but weaker ($r^2 < 0.2$, Table 2). No relationship was observed between $T_{VALLEY} - T_{MIDSLOPE}$ and daily-averaged wind-driven variables, including atmospheric pressure (Table 2).

Drainage flows mediate the effect of variable macro-climate on carbon fluxes

Because cold air drainage proceeded more readily under higher D, the models project that nocturnal RE in the valley is suppressed when mean daily D is high (relative to positions that do not experience cold air drainage, Fig. 6c). In contrast, little difference in the relationship between daytime RE and D is projected within and outside of the valley (Fig. 6d). As the predicted trends in GEP were also similar for both locations (Fig. 6d), differences in the daily integrated NEP are expected to be driven principally by differences in nighttime RE.

Direct observations of nocturnal and daytime NEP highlight that while the simple model failed to capture the magnitude of the observed variation in NEP, it predicted the direction of trends well. In particular, observed nocturnal NEP decreased with increasing D

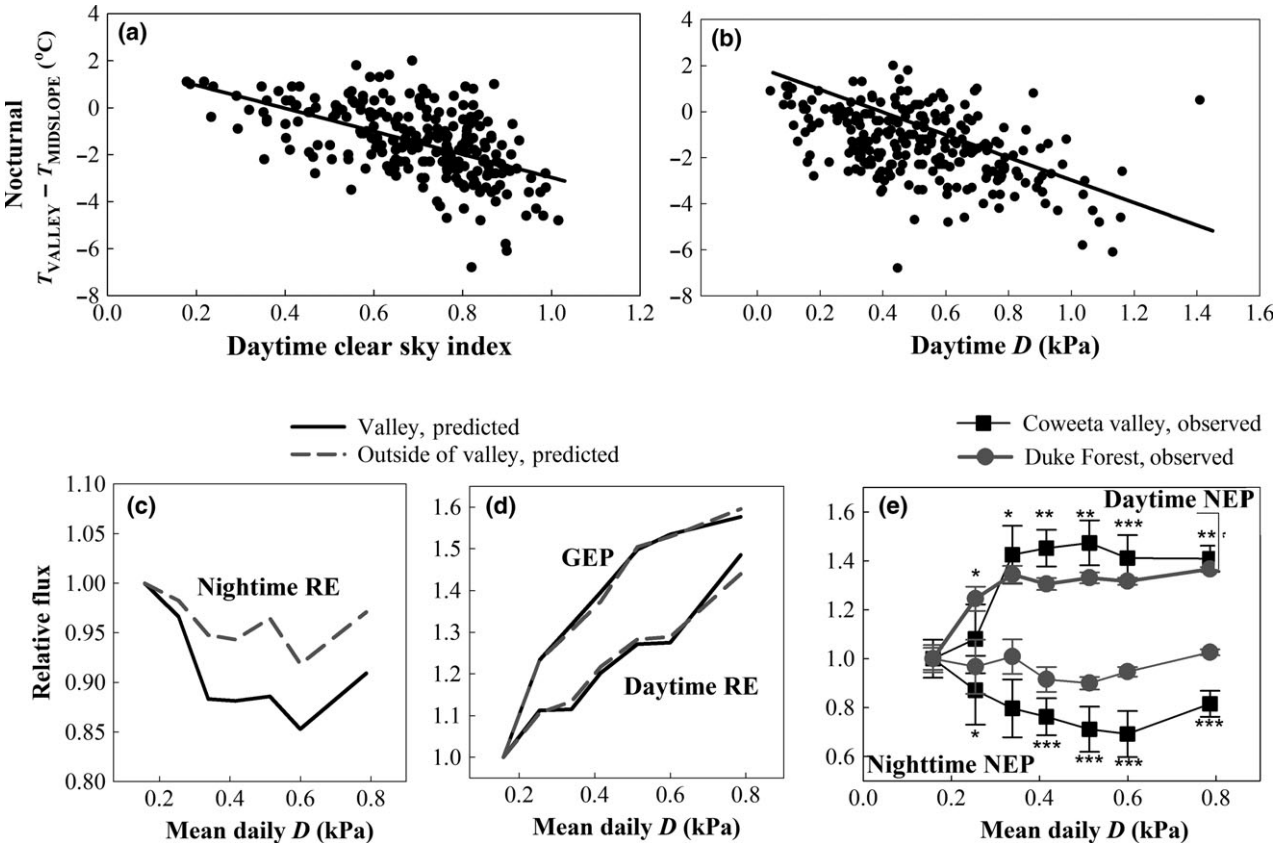

Fig. 6 The mean nocturnal (sunset–sunrise) temperature difference between the valley and mid-slope position, averaged over each night in the study period, as a function of the mean clear sky index (CSI, $P < 0.0001$, $r^2 = 0.3$, panel a) or mean daily vapor pressure deficit (D, $P < 0.0001$, $r^2 = 0.23$, panel b) observed during the 24-h period preceding sunrise. Panels (c) and (d) show the predicted change in ecosystem respiration (RE) and gross ecosystem productivity GEP as mean daytime vapor pressure deficit (D) increases inside (black lines) and outside (gray lines) of the valley. Panel (e) shows trends in the observed nighttime and daytime NEP observed at the Coweeta flux tower (black squares) or the Duke Forest flux tower (gray circles). Error bars show the standard error of the mean, and asterisks indicate whether the difference between the two sites is significant at the level of $0.001 < P < 0.05$ (*), or at the level of $P < 0.001$ (**).

Table 2 A characterization of the linear relationships between the difference in growing season nocturnal temperature observed in the valley position and the mid-slope position (i.e., $T_{VALLEY} - T_{MIDSLOPE}$) and assorted meteorological drivers. The $T_{VALLEY} - T_{MIDSLOPE}$ represents a proxy for cold air drainage intensity. Data were averaged to a daily timestep, with nocturnal data averaged from 2000 to 700 h on the following day. Other variables were averaged over the course of the day preceding each nocturnal period. The *P*-value results form a two-tailed Student's t-test for differences in the mean. The r^2 is the correlation coefficient

Variable	*P*	r^2	Slope
Incident short-wave radiation (R_g)	<0.0001	0.16	−0.009
Vapor pressure deficit (*D*)	<0.0001	0.23	−3.01
Clear sky index (CSI)	<0.0001	0.30	−4.91
Air temperature	0.023	<0.05	−0.073
Wind speed	No relationship		
Atmospheric pressure	No relationship		
Incident long-wave radiation	<0.0001	0.15	0.026
Friction velocity	No relationship		
Incident – outgoing – long-wave radiation	<0.001	0.34	0.056

in the Coweeta valley, but not the Piedmont site (Fig. 6e). Further, in both sites, daytime NEP was enhanced under higher *D*, but with larger relative increases in the Coweeta valley most of the time (Fig. 6e)

Discussion

Cold air drainage flows occurred frequently during the growing season, promoting temperature inversions characterized by nocturnal valley temperatures that were on average ~2 °C cooler, and occasionally more than ~5 °C cooler, than the midslope position (Fig. 2c). Our results demonstrate that the effect of cold air drainage on microclimate variables is not limited to nighttime periods, but rather is evident for several hours after sunrise and before sunset (Fig. 2), consistent with other work (Lundquist & Cayan, 2007). The decoupling between temperature in the valley as compared to the region at large confirms these results; while air temperature was usually lower in the Coweeta valley than the broader region, it was particularly low at night (Fig. 2d).

By driving models for RE and GEP with meteorological time series from the valley and region at large, we demonstrated that reductions to valley air temperature driven by cold air drainage reduced growing season averaged respiration by ~8.1% (ranging from 4.5–13%). Because drainage effects on GEP were negligible, this reduction to RE amounted to an enhancement to carbon uptake estimated to be ~10% during the growing season, and even higher (10–27%) on an annual basis.

Nocturnal cold air drainage proceeded more readily following low-humidity, clear days (Table 2, Fig. 6a, b), consistent with other studies (Barr & Orgill, 1989; Gudiksen *et al*., 1992). Thus, the correlation between enhanced nocturnal cooling in the valley and high *D* led to decreases in valley RE along a gradient of increasing *D*. This is a counterintuitive result that is neither observed nor predicted in the Piedmont site (Fig. 6e), where dry growing season periods often correspond with increases in nocturnal temperature, *D*, and respiration even during mild drought conditions (Novick *et al*., 2015). Because drainage flows had a negligible effect on GEP, the relatively low valley RE during dry periods corresponded to overall greater valley |NEP| when *D* was high. As much of the continental U.S. is expected to become drier in the future (Cook *et al*., 2015), the enhancements in cold air drainage on low-humidity days, and the impact of these enhancements on carbon fluxes in montane valleys, may represent a significant climate feedback.

Drainage flows in flux tower studies have been identified previously, but the inference space is limited to the challenges of interpreting tower-derived fluxes. Our efforts here possible due to a number of recent advancements in our ability to confidently interpret eddy covariance observations in complex terrain (Lee & Hu, 2002; Mammarella *et al*., 2007; Leuning *et al*., 2008; Feigenwinter *et al*., 2010; Novick *et al*., 2014). Nonetheless, biases in the flux data related to the complexity of the terrain may still persist, which injects some degree of uncertainty in our results.

The complimentary analysis of drainage flow effects on soil and leaf respiration, which relies on models developed using independent, chamber-based flux observations, gives us confidence that our results are not simply an observational bias. We inferred reductions to nocturnal R_{soil} and R_{leaf} on the order of 5% and 20%, respectively (Fig. 5c, d). If R_{soil} is assumed to be ~70% of total ecosystem respiration, consistent with previous estimates from a range of other eastern U.S. forests (Schafer *et al*., 2003; Wayson *et al*., 2006; Giasson *et al*., 2013; Novick *et al*., 2015), and the R_{leaf} modeled here is assumed to be representative of all aboveground biomass, then the reductions in nocturnal RE predicted from the leaf- and plot-level data amount to 0.7(0.95) + 0.3(0.8) = 0.095, or 9.5%. This is similar to the relative reductions inferred from the ecosystem-scale tower data (8.0%). We stress that this simple calculation serves principally to confirm that the inferred ecosystem-scale drainage flow effects are of a reasonable

magnitude, and does not represent a rigorous upscaling in space and/or time.

The analysis of soil and leaf respiration dynamics also allowed us to draw two important conclusions about the mechanisms underlying drainage flow effects on ecosystem respiration. First, we demonstrated that air temperature is much more variable than soil temperature, and more tightly coupled to changes in the cold air drainage regime over short (i.e., hourly to daily) time steps. Thus, the predicted and observed reductions to ecosystem respiration on clear, cloud-free days are most likely driven by reductions to leaf respiration. Second, by leveraging previously published estimates describing how R_{ref} and Q vary with elevation, we were able to show how acclimative adjustments to these parameters might affect the relative respiration rates between the valley and midslope positions. We estimate that these acclimative effects are relatively small, except for the case of daytime leaf respiration (Fig 5c, d), which may reflect that fact that acclimation in complex terrain is challenged by the fact that lapse rates are generally positive during the daytime, but often negative at night (i.e., see Fig 1).

Other important environmental variables can change with topographic position in ways that are relevant to this study, including soil moisture and atmospheric CO_2 concentration. As we were principally interested in isolating the effects of cold air drainage on carbon fluxes via its effects on temperature and D, we limited most of our analysis to a relatively narrow range of soil moisture in both the Coweeta and Duke Hardwood sites. However, we note that our results are largely unchanged even if that filter is removed, which would suggest that soil moisture plays a smaller role in limiting ecosystem respiration in this biome. This conclusion is supported by previous work showing that soil moisture limits soil respiration in the Coweeta basin by <3% (Nuckolls *et al.*, 2009), and that soil moisture limits ecosystem respiration in the Duke Hardwood site only during especially severe and rarely occurring drought events (Novick *et al.*, 2015). GEP is generally more sensitive to declining soil moisture than respiration (Ciais *et al.* 2003, Novick *et al.*, 2015). However, as the Coweeta Basin receives considerably more precipitation than other parts of the region (between 1800 and 3000 mm, Laseter *et al.*, 2012), it is unlikely that interactions between cold air drainage, temperature, and soil moisture during drought events would cause net carbon uptake to be more strongly reduced in the valley when compared to the region at large. Nonetheless, we certainly view this as a hypotheses worth testing, as previous work demonstrates that interactions between soil moisture, temperature, and macroclimate in complex terrain can produce surprising results (Vesala *et al.*, 2009; Crimmins *et al.*, 2011), and may be amplified in more xeric biomes

With respect to atmospheric CO_2, cold air drainage enhances CO_2 within and above the canopy during the nighttime and occasionally during early-to mid-morning (Novick *et al.*, 2014). These enhancements to CO_2 concentration could impact early morning photosynthesis in interesting ways which our data did not permit us to explore in detail in this particular study.

Finally, while cold air drainage clearly suppresses nocturnal temperature, and thus respiration, in valley positions, it is possible that cold air drainage may enhance temperature, and thus respiration, in upslope positions. As illustrated in Fig. 2e, the nocturnal temperature at the midslope position, when compared to the regional at large, is elevated at night over that predicted from the wet adiabatic lapse rate (~−2 °C). However, the same result was not observed for all climate stations in the basin (see SI), where in some locations nocturnal temperature was well aligned with that predicted from lapse rate effects. Even if a basin wide enhancement to nocturnal RE at higher elevations did exist, it would be compensated by reductions to daytime RE driven by lapse rate effects (see Fig. 2e and the SI), as well as potential enhancements to GEP associated with relatively lower daytime D in upslope positions. Our data do not allow us to fully disentangle all of these compensatory effects across the entire basin, although our results certainly motivate additional work to explore these interactions.

In summary, our work shows that frequent cold air drainage in the Coweeta valley suppressed growing season RE by ~8.1% (Figs 3 and 4), but had little effect on GEP, leading to enhancements of carbon uptake that were >10% and >15% on a growing season and annual basis, respectively, via mechanisms that are not well represented in terrestrial ecosystem models (Rotach *et al.* 2014). We also show that drainage flows evolve more easily on clear, low-humidity days (Fig. 6), such that nocturnal RE in the valley position *decreases*, and |NEP| increases, with increasing D. Given that D and solar radiation are variables that change significantly during drought periods (Oishi *et al.*, 2010), our results imply that cold air drainage could buffer valley forest NEP from the effects of droughts, which are expected to increase in frequency and severity under climate change (Cook *et al.*, 2015). This work should motivate further efforts to explore and model how cold air drainage and other physiographic processes might decouple local climate from macroscale conditions in ways that have significant effects on eco-physiological functioning.

Acknowledgements

The authors thank C. Sobek and S. Laseter for assistance with data collection and archiving, and P. Bolstad for providing valuable feedback on an early version of the manuscript. We thank W. Swank, J. Vose, L. Swift, and many other Coweeta Hydrologic Laboratory scientists for the dedicated efforts to support the long-term operation of the climate stations and the installation of the Coweeta Hydrologic Lab flux tower. Funding for the work was provided by the USDA Forest Service Southern Research Station and the NSF Long-Term Ecological Research (LTER) program (DEB-0823293 and DEB-1440485). We are grateful for the data provided by the NC CHRONOS database, a product of the State Climate Office of North Carolina, and for the data provided by the US Climate Reference Network, which is managed and maintained by the National Oceanic and Atmospheric Administration's (NOAA) National Centers for Environmental Information. The authors state they have no financial conflict of interest in the results of this study.

References

Ashcroft MB, Gollan JR (2012) Fine-resolution (25 m) topoclimatic grids of near-surface (5 cm) extreme temperatures and humidities across various habitats in a large (200 × 300 km) and diverse region. *International Journal of Climatology*, **32**, 2134–2148.

Aubinet M, Feigenwinter C, Heinesch B *et al.* (2010) Direct advection measurements do not help to solve the night-time CO_2 closure problem: evidence from three different forests. *Agricultural and Forest Meteorology*, **150**, 655–664.

Barr S, Orgill MM (1989) Influence of external meteorology on nocturnal valley drainage winds. *Journal of Applied Meteorology*, **28**, 497–517.

Bentz BJ, Logan JA, Amman GD (1991) Temperature-dependent development of the mountain pine beetle (Coleoptera: Scolytidae) and simulation of its phenology. *The Canadian Entomologist*, **123**, 1083–1094.

Bernacchi CJ, Pimentel C, Long SP (2003) In vivo temperature response functions of parameters required to model RuBP-limited photosynthesis. *Plant Cell and Environment*, **26**, 1419–1430.

Blennow K, Lindkvist L (2000) Models of low temperature and high irradiance and their application to explaining the risk of seedling mortality. *Forest Ecology and Management*, **125**, 289–301.

Bolstad PV, Swift L, Collins F, Regniere J (1998) Measured and predicted air temperatures at basin to regional scales in the southern Appalachian mountains. *Agricultural and Forest Meteorology*, **91**, 161–176.

Bolstad PV, Mitchell K, Vose JM (1999) Foliar temperature-respiration response functions for broad-leaved tree species in the southern Appalachians. *Tree Physiology*, **19**, 871–878.

Chung U, Seo HH, Hwang KH, Hwang BS, Choi J, Lee JT, Yun JI (2006) Minimum temperature mapping over complex terrain by estimating cold air accumulation potential. *Agricultural and Forest Meteorology*, **137**, 15–24.

Ciais Ph, Reichstein R, Viovy N *et al.* (2003) Europe-wide reduction in primary productivity caused by the heat and drought in 2003. *Nature*, **437**, 529–533.

Cook BI, Ault TR, Smerdon JE (2015) Unprecedented 21st century drought risk in the American Southwest and Central Plains. *Science Advances*, **1**, e1400082.

Cox HJ (1920) Weather conditions and thermal belts in the North Carolina Mountain Region and their relation to fruit growing. *Annals of the Association of American Geographers*, **10**, 57–68.

Crimmins SM, Dobrowski SZ, Greenberg JA, Abatzoglou J, Mynsberge AR (2011) Changes in climatic water balance drive downhill shifts in plant species' optimum elevations. *Science*, **331**, 324–327.

Daly C (2006) Guidelines for assessing the suitability of spatial climate data sets. *International Journal of Climatology*, **26**, 707–721.

Daly C, Conklin DR, Unwsorth MH (2010) Local atmospheric decoupling in complex topography alters climate change impacts. *International Journal of Climatology*, **30**, 1857–1864.

Dobrowski SZ (2011) A climatic basis for microrefugia: the influence of terrain on climate. *Global Change Biology*, **17**, 1022–1035.

Feigenwinter C, Montagnani L, Aubinet M (2010) Plot-scale vertical and horizontal transport of CO_2 modified by a persistent slope wind system in and above an alpine forest. *Agricultural and Forest Meteorology*, **150**, 665–673.

Gan JB (2004) Risk and damage of southern pine beetle outbreaks under global climate change. *Forest Ecology and Management*, **191**, 61–71.

Giasson M-A, Ellison AM, Bowden R *et al.* (2013) Soil respiration in a northeastern US temperate forest: a 22-year synthesis. *Ecosphere*, **4**, art140.

van Gorsel E, Delpierre N, Leuning R *et al.* (2009) Estimating nocturnal ecosystem respiration from the vertical turbulent flux and change in storage of CO_2. *Agricultural and Forest Meteorology*, **149**, 1919–1930.

Gudiksen PH, Leone JM, King CW, Ruffieux D, Neff WD (1992) Measurements and modeling of the effects of ambient meteorology on nocturnal drainage flows. *Journal of Applied Meteorology*, **31**, 1023–1032.

Holden ZA, Abatzoglou JT, Luce CH, Baggett LS (2011) Empirical downscaling of daily minimum air temperature at very fine resolutions in complex terrain. *Agricultural and Forest Meteorology*, **151**, 1066–1073.

Hubbart JA, Kavanagh KL, Pangle R, Link T, Schotzko A (2007) Cold air drainage and modeled nocturnal leaf water potential in complex forested terrain. *Tree Physiology*, **27**, 631–639.

Inouye DW, Barr B, Armitage KB, Inouye BD (2000) Climate change is affecting altitudinal migrants and hibernating species. *Proceedings of the National Academy of Sciences of the United States of America*, **97**, 1630–1633.

Juang J-Y, Katul G, Siqueira M, Stoy P, Novick K (2007) Separating the effects of albedo from eco-physiological changes on surface temperature along a successional chronosequence in the southeastern United States. *Geophysical Research Letters*, **34**, L21408, doi:10.1029/2007GL031296 .

Kapos B, Rhind J, Edwards M, Price M, Ravilious C, Burt N (2000) Developing a map of the world's mountain forests. In: *Forests in Sustainable Mountain Development: A State of Knowledge Report for the 2000 Task Force on Forests in Sustainable Mountain Development* (eds Price MF, Butt N), pp. 4–19. Cabi Publishing, Oxfordshire, UK.

Kramer K, Leinonen I, Loustau D (2000) The importance of phenology for the evaluation of impact of climate change on growth of boreal, temperate and Mediterranean forests ecosystems: an overview. *International Journal of Biometeorology*, **44**, 67–75.

Laseter SH, Ford CR, Vose JM, Swift LW (2012) Long-term temperature and precipitation trends at the Coweeta Hydrologic Laboratory, Otto, North Carolina, USA. *Hydrology Research*, **43**, 890–901.

Lasslop G, Reichstein M, Papale D *et al.* (2010) Separation of net ecosystem exchange into assimilation and respiration using a light response curve approach: critical issues and global evaluation. *Global Change Biology*, **16**, 187–208.

Lee XH, Hu XZ (2002) Forest-air fluxes of carbon, water and energy over non-flat terrain. *Boundary-Layer Meteorology*, **103**, 277–301.

Leuning R, Zegelin SJ, Jones K, Keith H, Hughes D (2008) Measurement of horizontal and vertical advection of CO_2 within a forest canopy. *Agricultural and Forest Meteorology*, **148**, 1777–1797.

Long S (1991) Modification of the response of photosynthetic productivity to rising temperature by atmospheric CO2 concentrations – has its importance been underestimated? *Plant Cell and Environment*, **14**, 729–739.

Lundquist JD, Cayan DR (2007) Surface temperature patterns in complex terrain: daily variations and long-term change in the central Sierra Nevada, California. *Journal of Geophysical Research-Atmospheres*, **112**, D11124, doi:10.1029/2006JD007561.

Luyssaert S, Jammet M, Stoy PCS *et al.* (2014) Land management and land cover change have impacts of similar magnitude on surface temperature. *Nature Climate Change*, **4**, 389–393.

Mahrt L, Vickers D, Nakamura R, Soler MR, Sun JL, Burns S, Lenschow DH (2001) Shallow drainage flows. *Boundary-Layer Meteorology*, **101**, 243–260.

Mammarella I, Kolari P, Rinne J, Keronen P, Pumpanen J, Vesala T (2007) Determining the contribution of vertical advection to the net ecosystem exchange at Hyytiälä forest, Finland. *Tellus Series B*, **59**, 900–909.

Mitchell KA, Bolstad PV, Vose JM (1998) Interspecific and environmentally induced variation in foliar dark respiration among eighteen southeastern deciduous tree species. *Tree Physiology*, **19**, 861–870.

Novick KA, Walker JT, Chan WS, Sobek CM, Vose JM (2013) Eddy covariance measurements with a new fast-response, closed-path analyzer: spectral characteristics and cross-system comparisons. *Agricultural and Forest Meteorology*, **181**, 17–32.

Novick KA, Brantley ST, Miniat CF, Walker J, Vose J (2014) Inferring the contribution of advection to total ecosystem scalar fluxes over a tall forest in complex terrain. *Agricultural and Forest Meteorology*, **185**, 1–13.

Novick KA, Oishi AC, Ward EJ, Siqueira MBS, Juang J-Y, Stoy PC (2015) On the difference in the net ecosystem exchange of CO_2 between deciduous and evergreen forests in the southeastern U.S. *Global Change Biology*, **21**, 827–842.

Nuckolls AE, Wurzburger N, Ford CR, Hendrick RL, Vose JM, Kloeppel BD (2009) Hemlock declines rapidly with hemlock woolly adelgid infestation: impacts on the carbon cycle of southern Appalachian forests. *Ecosystems*, **12**, 179–190.

Oishi AC, Oren R, Novick KA, Palmroth S, Katul GG (2010) Interannual invariability of forest evapotranspiration and its consequence to water flow downstream. *Ecosystems*, **13**, 421–436.

Pypker TG, Unsworth MH, Mix AC, Rugh W, Ocheltree T, Alstad K, Bond BJ (2007) Using nocturnal cold air drainage flow to monitor ecosystem processes in complex terrain. *Ecological Applications*, **17**, 702–714.

Reichstein M, Katterer T, Andren O *et al.* (2005) Temperature sensitivity of decomposition in relation to soil organic matter pools: critique and outlook. *Biogeosciences*, **2**, 317–321.

Rotach MW, Wohlfahrt G, Hansel A, Reif M, Wagner J, Gohm A (2014) The world is not flat: implications for the global carbon balance. *Bulletin of the American Meterological Society*, **95**, 1021–1028.

Schafer KVR, Oren R, Ellsworth DS *et al.* (2003) Exposure to an enriched CO2 atmosphere alters carbon assimilation and allocation in a pine forest ecosystem. *Global Change Biology*, **9**, 1378–1400.

Stoy PC, Katul GG, Siqueira MBS *et al.* (2008) Role of vegetation in determining carbon sequestration along ecological succession in the southeastern United States. *Global Change Biology*, **14**, 1409–1427.

Thuiller W, Lavorel S, Araujo MB, Sykes MT, Prentice IC (2005) Climate change threats to plant diversity in Europe. *Proceedings of the National Academy of Sciences of the United States of America*, **102**, 8245–8250.

Tjoelker MG, Oleksyn J, Reich PB (2001) Modelling respiration of vegetation: evidence for a general temperature-dependent Q_{10}. *Global Change Biology*, **7**, 223–230.

Vesala T, Launiainen S, Kolari P *et al.* (2009) Autumn warming and carbon balance of a boreal Scots pine forest in Southern Finland. *Biogeosciences Discussions*, **6**, 7053–7081.

Wayson CA, Randolph JC, Hanson PJ, Grimmond CSB, Schmid HP (2006) Comparison of soil respiration methods in a mid-latitude deciduous forest. *Biogeochemistry*, **80**, 173–189.

Weyman DR (1973) Measurements of the downslope flow of water in a soil. *Journal of Hydrology*, **20**, 267–288.

Yi CX, Anderson DE, Turnipseed AA, Burns SP, Sparks JP, Stannard DI, Monson RK (2008) The contribution of advective fluxes to net ecosystem exchange in a high-elevation, subalpine forest. *Ecological Applications*, **18**, 1379–1390.

Supporting Information

Additional Supporting Information may be found in the online version of this article:

Appendix S1. Micro-climate dynamics within the Coweeta Basin inferred from a broader set of climate stations.
Figure S1. The location of the five long-running climate stations in the Coweeta Basin.
Figure S2. The mean hourly growing season temperature difference between CS01 and the other four climate stations within the basin.
Figure S3. The mean daily nocturnal temperature difference between CS01 and the other four stations in the network as a function of the mean daily vapor pressure deficit (*D*) recorded at CS01 on the preceding day.
Figure S4. The mean hourly growing season temperature difference between Climate Stations 17, 21, 8 and 77 and the region at large.
Appendix S2. Characteristics of meteorological stations used in the regional analysis, and quality control of those data: All meteorological stations used in the study are described in Table S2
Table S2. Characteristics of the meteorological stations.
Figure S5. The mean hourly difference in growing season temperature between CS01 and the USCRN stations only.
Appendix S3. Calculating the clear sky index.
Appendix S4. The energy balance model to determine the temperature changes attributable to differences in solar radiation between the Coweeta basin and the broader region.
Figure S6. The mean hourly incident growing season shortwave radiation (left-panel) and incident long-wave radiation (right panel) measured on the Coweeta flux tower.